THE ATMOSPHERE OF MERCURY

by

S. I. RASOOL

Goddard Space Flight Center,
Institute for Space Studies, NASA,
New York, New York

and

New York University,
Department of Meteorology and Oceanography,
New York, New York

S. H. GROSS

Airborne Instruments Laboratory,
Melville, New York

W. E. McGOVERN

New York University,
Department of Meteorology and Oceanography, :
New York, New York

January 1966

CONTENTS

1. INTRODUCTION

Mercury is the smallest planet of the solar system
and is also nearest to the sun. The combination of these
two circumstances makes it a hot and gravitationally "weak"
planet. It has therefore been a firm belief that any at-
mosphere which the planet could have acquired during its
formation and/or by the subsequent outgassing processes
would be difficult to hold. High thermal velocities of the
particles in the atmosphere would win over the relatively
small escape velocity and therefore, shortly after its
formation, the planet would lose practically all its at-
mosphere to the space.

In the literature on planets, the description of the
atmosphere of Mercury has usually been very brief (e.g.,
Kuiper, 1952; Urey, 1959; Dollfus, 1961), and Mercury has
invariably been compared with the moon, as a planet without
an atmosphere. In the last few years, however, evidence
has accumulated that the atmosphere of Mercury may not be,
after all, as tenuous as that of the moon, but could have
a surface pressure of as much as 1 - 10 mb, at least 10^{10}
times greater than at the surface of the moon. This has
been further substantiated by the recent identification of

a small amount of CO_2 in the atmosphere of Mercury (Moroz, 1963, 1965).

Also, the recent radar investigations of the planet (Pettengill and Dyce, 1965) have led to the remarkable discovery that Mercury is not in synchronous rotation but, instead, rotates much faster, with a period of 59 ± 5 days.

It is the purpose of this paper to review the available information on the temperature, composition, and surface pressure of Mercury's atmosphere, to discuss the implications of a non-synchronous rotation of the planet on the atmosphere. We construct several models for the atmosphere which are consistent with the observations in an attempt to determine if they are stable against depletion of the atmosphere by gravitational escape. The results are discussed from the standpoint of the surface of the atmosphere.

2. ROTATION

2.1 Early Visual Observations of the Planet

The first telescopic observations of Mercury, leading to the discovery of the phases of the planet, were carried out by Zupus in 1639. Because Mercury is small, distant, and is never more than 28° of arc away from the sun, it is extremely difficult to observe, being only visible low on

the horizon in the very early hours of twilight. It is

for this reason that it was not until 1882 that the first

reliable map of the planetary disk was drawn. Schiaparelli

had then conceived the idea of observing the planet in the

daytime. But because of this inherent difficulty in ob-

serving the planet, the data on Mercury, even to this day,

remains extremely meager.

The drawing of Mercury made by Schiaparelli (1889) showed

irregular dark markings on the surface of the planet which,

after subsequent observations, were found to be of a perma-

nent nature. Antoniadi (1934), after an extensive series of

observations, produced the first planisphere of the day-side

of the planet. Lyot (1943) and Dollfus (1953) continued

such observations of Mercury and produced a series of drawings

which have been discussed in detail by Dollfus (1961).

From the first observations, it was noticed that when

the planet was continually observed over a period of several

hours, the markings did not shift across the disk. This led

Schiaparelli to conclude that Mercury must have a synchronous

rotation, spinning on its axis in 88 days which is also the

time of its orbital revolution. When later observations re-

vealed a recurrence of the markings, even over long intervals

of time, it led practically all observers to conclude that

Mercury had a rotation synchronous with its revolution. This conclusion was further substantiated by the theoretical argument that because of the nearness of the planet to the sun, the solar tidal forces would be so strong that they would slow down the rotation of Mercury in the very early history of the solar system. Like the moon with respect to the earth, Mercury would be "locked" in the direction of the sun.

2.2 Recent Radar Measurements

During the inferior conjunction of Mercury in April, 1965, Pettengill and Dyce (1965) made radar observations of the planet and derived a value for the rotation period of 59 ± 5 days. Figure 1 shows their results of the limb-to-limb doppler spread as a function of time for four measurements taken during the months of March and April, 1965. The best fit curve indicates direct rotation with the sidereal period of 59 ± 5 days. The authors have also pointed out that the direction of the pole may be normal to the planetary orbit.

This new result is in complete disagreement with the hitherto widely accepted value of 88 days, derived from the visual observations as discussed in the previous section.

McGovern, Gross and Rasool (1965) have investigated the
reasons for this apparent inconsistency between the results
of the early visual observations and the recent radar
measurements. Nearly 50 drawings of Mercury published by
Lowell (1902), Antoniadi (1934), Lyot (1943), Dollfus (1961)
and Baum (see Sandner, 1963 and Moore, 1960) were examined.
Of these, six pairs of drawings showed near duplication of
markings and phase. These pairs are listed in Table I.

TABLE I

	Time interval T (in days)
1. Antoniadi (Aug. 11,1924) and Antoniadi (June 21,1927)	1044
2. Antoniadi (Aug. 23,1927) and Antoniadi (Aug. 6,1928)	349
3. Antoniadi (Oct. 4,1927) and Antoniadi (Aug. 23,1929)	690
4. Antoniadi (Aug. 6,1928) and Antoniadi (July 20,1929)	348
5. Lyot (July 22,1942) and Dollfus (Oct. 12,1950)	3004
6. Baum (March 15,1952) and Baum (March 1,1953)	351

The authors pointed out that duplication of markings and
phase for any single pair of drawings of Mercury does not
necessarily indicate that synchronous rotation of the planet
is the only possible solution. A number of other periods of
rotation are possible as given by the following equation:

- 5 -

$$P = \frac{T}{n + \dfrac{\theta}{360}}$$

where P is the period of rotation of Mercury in days, T the
time interval between the two observations made at the same
phase, n the number of complete rotations of the planet during
this time interval and θ the average angular displacement of
the earth and Mercury in their orbits. Figure 2 shows all
possible values of P between 40 and 90 days as calculated for
each pair of drawings. It is noted that in addition to an 88-
day period, there are at least four more values of P, viz.,
43.6, 50.1, 58.4 and 70.2 days which will be consistent with
all the six pairs of drawings. However, only one of these
values is within the allowed limits of 59 ± 5 days determined
by radar. Therefore the rotation period of 58.4 ± 0.5 days
is consistent with both the visual and the radar observations
of Mercury.

If, however, we take only the pair number 5, which has
the longest time interval and also the most convincing dupli-
cation of markings, we can narrow down the accuracy limits to
a value of 58.65 ± 0.10 days.

Peale and Gold (1965) have made an interesting analysis
of the problem and have explained the non-synchronous rota-
tion of Mercury by the following simple argument. The el-
lipticity of the orbit of Mercury around the sun is very

large, about 0.2. The tidal torque is proportional to $1/r^6$ and will be greatest at the perhelion. The planet can therefore acquire a rotation period lying between 56.6 and 88 days, depending on the dissipation function of the tidal forces. If the value of 58.65± 0.1 days, as derived above, is correct, then following Peale and Gold's argument, it will indicate that there is a significant amplitude dependence of the tidal dissipation on Mercury.

Another argument in favor of the 58.6 day period has been advanced by Colombo (1965), who suggests that a period of rotation which is exactly 2/3 of the orbital period will be stable because such a rotation period will bring the axis of minimum moment of inertia in line with the sun-Mercury radius vector at every perhelion. However, based on only this line of argument, one can obtain a large number of "stable" rotation periods for Mercury. Combining such an analysis with the arguments given by Peale and Gold and also with the radar and visual observations, one can finally obtain a precise value for the rotation, viz. 58.65 days.

The non-synchronous rotation of Mercury implies, contrary to the previous belief, that all parts of the planet are exposed to the sun at one time or another. The length of the day on Mercury is approximately 176 earth days, and

it may be a fair assumption that the surface temperature on the night side of the planet may, after all, not be as low as 28 $^\circ$K which was calculated by Walker (1961) for a synchronously rotating planet.

3. EVIDENCE FOR THE PRESENCE OF AN ATMOSPHERE ON MERCURY

The astronomical constants of the planet Mercury are summarized in Table II.

<u>TABLE II</u>

MASS	0.054 (Earth 1)
RADIUS	0.39 (Earth 1)
DENSITY	5.05 gm/cm^3
$V_c = \sqrt{\dfrac{2MG}{R}}$	4.2 km/sec (Earth 11.3 km/sec)
g	350 cm/sec^2
DISTANCE FROM SUN	0.39 A.U.
SOLAR RADIATION FLUX	6.6 x at Earth
ALBEDO	0.07 (Earth 0.4)
T_e (sub-solar point)	616 $^\circ$K
ORBITAL PERIOD	88^d
ROTATION	58.65 ± 0.1^d

3.1 Polarimetric Studies

One of the most important techniques of studying the surface of another planet is the observation of the polarization of solar radiation reflected by the planet. This technique was developed by Lyot (1929) and has since been used extensively by him and later by Dollfus to study the surfaces of the moon and planets. A detailed discussion of this method is given by Dollfus (1957, 1961, and 1962).

One of the by-products of such an observation is an estimate of the total atmosphere of the planet. By comparing the polarization of the solar radiation as reflected from the center of the planetary disk and from the limb, one can obtain an estimate of the scattering of the radiation by the atmosphere. Making such measurements at different wavelengths and assuming Rayleigh scattering to be the main process, one can estimate the total number of molecules in the atmosphere. In this manner, Lyot (1929) gave an upper limit on the extent of the atmosphere of Mercury, viz., < 21/1000 of the earth's atmosphere. For the smaller value of g for Mercury, this would correspond to a pressure of 7 mb. In these calculations, it was assumed that the albedo

of Mercury, in the visible, was 0.16. The recent measurements by Harris (1961) give a value of 0.063. If we correct Lyot's calculations for this new value of albedo, we obtain an upper limit on the surface pressure on Mercury of 3 mb. Dollfus repeated Lyot's observations with an improved polarimeter and using the same method of reduction of data, gave a value of the atmospheric pressure at the surface of Mercury equal to 1 mb within an order of magnitude, i.e., $P_S = 10^{0\pm1}$.

It is difficult to accept the results without qualifications because of the inherent limitations of this method in deducing the atmospheric pressure. The most important source of error is the assumption that the scattering is entirely molecular. Any particulate matter which may be present in the atmosphere will result in a considerable over-estimate of the pressure. Also, it is assumed that the atmosphere of Mercury has the same scattering properties as air. If, however, the major component of the atmosphere of Mercury were not nitrogen but, for example, neon, the pressure quoted above would be an under-estimate by as much as a factor of 10. Chamberlain and Hunten (1965) have recently given a critical review of the inherent difficulties in this method for estimating the atmospheric pressure.

Accepting their arguments, we would conclude that the un-
certainty of an order of magnitude quoted by Dollfus may
be quite optimistic, and the actual atmospheric pressure
on the surface of Mercury may be anywhere between 0.01 and
10 mb.

3.2 Spectroscopic Studies

The search for atmospheric gases on Mercury was
carried out by Adams and Dunham (1932) and later by Kuiper
(1952), but failed to give any positive results. It was
therefore generally believed that if an atmosphere exists
on Mercury, it must be composed of rare gases, perhaps argon
(Field, 1964), not observable by spectroscopic techniques.
Recently, however, Moroz (1963) has detected the
presence of CO_2 in the atmosphere of Mercury. He recorded
the spectrum of solar radiation as reflected by Mercury and
compared it with that of the moon. The equivalent width of
the 1.6 μ CO_2 band appears enhanced in the Mercury spectrum,
indicating the presence of CO_2 in the atmosphere of the
planet. This is illustrated in Figure 3. A series of
similar measurements, however, show a lesser enhancement
of the equivalent width (Moroz, 1965).

As the strengths of the saturated CO_2 lines in the

1.6 μ band depend both on the effective pressure and the amount of CO_2, it is not possible to separate the two by observing only in this one band. Spinrad, Field and Hodge (1965), therefore, attempted to measure the intensity of the weak unsaturated lines of CO_2 at 8700Å which are not pressure-dependent. Combining these measurements with those of Moroz, they expected to get the amount of CO_2 and the total atmospheric pressure at the surface of the planet. Despite a detection limit of as low as 4 mÅ, they were unable to observe CO_2 lines in the 8700Å region. They therefore proposed an upper limit to the CO_2 content of 57 m-atm., which corresponds to a maximum possible partial pressure of 4.2 mb on the surface. Combining this upper limit on the amount of CO_2 with Moroz' observation of the equivalent width of the 1.6 μ CO_2 band, Spinrad, Field and Hodge conclude that the surface pressure on Mercury is near 4 mb if the atmosphere is pure CO_2, and higher if other gases are present.

Kozyrev (1964) observed Mercury during an eclipse of the sun and found emission lines of hydrogen in the spectrum. He therefore postulated that the atmosphere of Mercury may contain a significant amount of hydrogen. Spinrad and Hodge (1965) have given a more acceptable explanation of these

line profiles, suggesting that they could have been formed by a spurious blending of the doppler-shifted Fraunhofer lines in the spectrum of Mercury and the unshifted component in the sky spectrum.

In summary, it appears from the evidence described above that Mercury has a tenuous atmosphere, with a surface pressure between 1 and 10 mb and containing a small amount of CO_2.

4. TEMPERATURE MEASUREMENTS

For a slowly rotating planet like Mercury, the effective equilibrium temperature on the day side of the planet is given by

$$T_e \sim \left(\frac{F}{2\sigma} (1 - A) \right)^{1/4} \tag{2}$$

where F is the solar flux reaching Mercury (1.1×10^7 ergs/cm^2/sec) and A is the albedo (0.063) (Harris, 1961). For these values of F and A, the mean effective temperature of the day side of Mercury is 520 $^\circ$K. At the subsolar point the temperature will be 616 $^\circ$K. A tenuous atmosphere precludes any substantial greenhouse effect and therefore we can expect the surface temperature of the day

side to be approximately the same as the effective temperatures computed above.

Temperature measurements of Mercury have been made by recording the thermal emission of the planet in the infrared and microwave regions of the spectrum. We shall discuss the results of these two types of observations in the following paragraphs.

4.1 Infrared

Pettit (1961) has measured thermal emission from Mercury in the 8 - 12 μ region and obtains a sub-solar point surface temperature of 615 $^{\circ}$K, in close agreement with the effective temperature given above. This agreement between the observed surface and effective temperatures of the planet indicates that the surface of Mercury radiates as a black body in the far infrared with an emissivity of approximately unity.

4.2 Microwaves

Thermal radiation from Mercury in the microwave region at λ = 3 cm was measured by Howard, Barrett and Haddock (1962). Figure 4 shows their temperature values as a function of phase angle. The interesting feature of their results is

that the dependence of the temperature on the phase angle
is not so strong as would be expected if the dark side were
extremely cold, at a temperature close to 28 $^{\circ}$K (Walker,
1961).

Field (1964) interpreted these results to suggest that
the dark side of Mercury may actually be at a higher tem-
perature. Curve A in Figure 4 shows the variation of tem-
perature as a function of phase angle which would be ob-
served if the dark side were at a temperature as high as
300 $^{\circ}$K. The observed values of temperature show a better
agreement with curve A than with curve B which is computed
for a dark side at 0 $^{\circ}$K. Field also suggested that in or-
der to explain these observations, an atmosphere must be
present which would transport the heat required to raise
the temperature of the dark side to 300 $^{\circ}$K. This suggestion
of Field's is based on the assumption that the measured
radio brightness temperatures are actually the surface tem-
peratures of Mercury.

Mayer (1961) has however pointed out that the thermal
emission in the radio wavelengths originates a few wave-
lengths below the surface of the planet. More recent
radio measurements of Mercury by Kellerman (1965) at $\lambda = 11$ cm
corroborate this argument. Figure 5, taken from Kellerman,

does not show any phase effect at all, indicating that the temperature a few decimeters below the surface of Mercury may be constant at 300 $^\circ$K, both on the day and night sides. Now that it is known that the rotation of Mercury is non-synchronous, and that all parts of the planet are exposed to solar radiation every 88 days (one solar day on Mercury is equal to 176 earth days), a 300 $^\circ$K temperature in the sub-surface layers on the dark side of Mercury seems plausible.

No observational information is yet available on the actual surface temperature on the dark side of the planet, but Field has argued that if argon is present in the atmosphere, then the temperature of the surface of the dark side should be higher than 56 $^\circ$K so that the atmosphere does not freeze out. For a carbon dioxide atmosphere, this temperature should be higher than 150 $^\circ$K.

Mintz (1962) has made a theoretical study of the problem of heat transport across the terminator by winds, for a slowly rotating planet. Using his expression which relates t wind velocity at the terminator and the temperature on the dark side of the planet, we have made a sample calculation for the Mercurian atmosphere, mainly composed of CO_2, and for P_s = 5 mb. Figure 6 is a plot of the required wind

velocities as a function of temperature increase on the dark side of the planet. Also plotted is a curve giving the velocity of sound in the atmosphere at these temperatures. It appears that even in a thin atmosphere of 5 mb surface pressure, atmospheric circulation is an efficient means of transporting heat from the day side to the night side of the planet. A 120 m/sec wind can maintain the dark side of Mercury at 150 $^{\circ}$K, thus preventing CO_2 from freezing out. Wind velocities of the order of 100 m/sec are frequently observed in the upper atmosphere of the earth.

5. PROBLEM OF GRAVITATIONAL ESCAPE AND ACCUMULATION OF AN ATMOSPHERE

In this section we shall examine the processes which govern the evolution of an atmosphere on a small and hot planet like Mercury. There are two schools of thought on the problem of the origin of a planetary atmosphere.

It has been suggested that the present atmosphere is either (a) the remnant of a dense gaseous envelope which the planet may have acquired at the time of its accumulation out of the contracting solar nebula, or (b) the result of slow outgassing from the interior of the planet via, e.g., volcanic activity and the exhalation of gases through fissures in the crust.

For the present atmosphere to be the remnant of a primitive one, it must be stable against the two important loss processes: thermal escape of gases from the gravitational field of the planet, and the dissipative effect of the solar wind. The atmosphere, in this case, would be composed of those gases which have not yet escaped or been ejected by the solar wind. Their abundances would, therefore, still be in the same relative amounts as observed in

the sun.

On the other hand, it is difficult to ascertain if the present atmosphere of another planet is the result of outgassing. Even in the case of the earth, the gas exhalation rates from the crust are very poorly known and extrapolating these to other planets could be very unreliable. The volcanic outgassing not only depends on the differential processes and tectonic activity occurring in the interior of the planet, but also on the nature of "volatiles" which were trapped within the planet at the time of its formation. These are difficult questions in cosmogony and are beyond the scope of this paper.

We would like to point out that the major argument in favor of the outgassing hypothesis is the demonstration that the present atmosphere could not be primordial in origin.

For this purpose we shall discuss the problems of gravitational escape and the effect of solar wind in more detail, with particular reference to Mercury.

5.1 Thermal Escape

The flux of particles escaping from the top of a planetary atmosphere is readily estimated from the theory of Jeans (1916) as modified by Spitzer (1952). Neglecting

diffusion, the total number of escaping particles, F, is given by

$$F = \frac{4\pi R_o^2 \, n_{oi} \, CYe^{-Y}}{\sqrt{6\pi}} \left[\frac{R_c}{R_o} \left(1 + \frac{R_c}{YR_o} \right) \right] \text{ cm}^{-2} \text{ sec}^{-1} \quad (3)$$

where R_o is the radius of the planet, R_c is the planetary radius at the base of the exosphere, n_{oi} is the density which would exist at the surface of the planet if the atmosphere were isothermal at all heights, C is the root-mean-square velocity of the atmospheric particles, and

$$Y = \frac{GmM}{kT_c R_o} \, , \quad (4)$$

where m is the mass of the escaping constituent, M is the mass of the planet, G is the gravitational constant, and T_c is the temperature of the exosphere.

The number of escaping particles therefore particularly depends on the temperature at the top of the atmosphere, on the dimensions of the planet, and also on the molecular weight of the escaping particles. Using Eq. (3) we can calculate, for different values of T_c, the time in which the abundance of a gaseous constituent on Mercury would decrease to 1/e of its initial value, which is essentially the half-life of the constituent. The results

are plotted in Figure 7. The times of escape have been calculated for three different temperature values, viz., 500 ^{O}K, 1000 ^{O}K, and 2000 ^{O}K, and are plotted as a function of atomic or molecular weight of the escaping particles. For a planetary lifetime of 5×10^{9} years, it is seen that Mercury will lose all its hydrogen and helium at an exospheric temperature > 200 ^{O}K, but will retain atomic oxygen at $T_c < 800$ ^{O}K, and argon at $T_c < 1800$ ^{O}K. At temperatures higher than 2000 ^{O}K, only heavy gases like krypton and xenon could be retained by the planet.

Because Mercury is very close to the sun ($R \approx 0.4$ A.U.) and therefore receives 6.6 times more solar flux than the earth (Table II), one would expect the exospheric temperature to be much higher than for the earth (1500 ^{O}K). In fact, the values for T_c for Mercury quoted in the literature are as high as 5000 ^{O}K (Urey, 1959). According to Figure 7, at such a high temperature, even xenon will be lost, and one would not expect even a trace of an atmosphere on Mercury. For the atmosphere of Mercury to be stable against gravitational escape, the exospheric temperature should be considerably less than 5000 ^{O}K. From the table of solar and cosmic abundances (Cameron, 1963) the most

abundant molecules in a primitive atmosphere, after the escape of hydrogen and helium, would be carbon dioxide, neon and nitrogen. Their relative amounts by volume are given in Table III.

<div align="center">

TABLE III

COMPOSITION OF A PRIMITIVE ATMOSPHERE
AFTER THE ESCAPE OF H_2 AND He

</div>

CO_2	60 %
Ne	25 %
N_2	15 %
A	< 0.5 %

This table has been computed with the assumptions that: (1) all hydrogen and helium have completely escaped, including that hydrogen which could have been in the form of CH_4, NH_3, or H_2O; (2) the oxygen available for the atmosphere has been depleted by that amount which would be required to form metal oxides and silicates; (3) only that much carbon is included in the atmosphere which will combine with the remaining oxygen to form carbon dioxide; and (4) carbon dioxide has not been removed from the atmosphere by reactions with the crust of the planet.

In order for this atmosphere to be stable against

gravitational escape, the temperature of the exosphere of Mercury must be < 800 $^{\circ}$K (Fig. 7), which is the escape temperature for atomic oxygen, a dissociation product of carbon dioxide. If, on the other hand, the temperature of the exosphere is higher than 800 $^{\circ}$K, then, to maintain a carbon dioxide atmosphere on Mercury, a considerable amount of outgassing will be required to counter the high flux of escaping particles.

5.2 Solar Wind

Interactions between the solar wind and the atmosphere of Mercury may produce several important effects such as ejection of ionized particles, intense heating, and ionization in the upper atmosphere, and also accretion of constituents into the atmosphere. But these effects will be highly dependent on the extent and nature of the planetary magnetic field. In the absence of any information on the magnetic field of Mercury, we shall limit out discussion of this aspect of the problem to the derivation of a lower limit to the field strength which would protect the atmosphere of Mercury from the dissipative effects of the solar wind.

We shall assume that an effective protection of the atmosphere from the solar wind will be achieved if the

magnetic pressure at the height of the exosphere is greater than or equal to the dynamic pressure of the solar wind; that is, we set

$$\frac{B_c^2}{8\pi} \geq n\,m\,v^2 \qquad (5)$$

where B_c is the field strength at the boundary of the magnetosphere, which is assumed to be one planetary radius away from the surface and therefore above the exosphere, and n, m, and v are the number density, mass and velocity, respectively, of the particles in the solar wind. Extrapolating the flux data obtained from Mariner II to the distance of Mercury, we find that $n \sim 100/cm^3$ and $v \sim 5 \times 10^7$ cm/sec. This gives $B_c \sim 300\,\gamma$ at one planetary radius away from the surface. The dipole field at the surface will then be 0.024 gauss. This is approximately 20 times less than the magnetic field strength of the earth.

The real problem of interaction of the solar wind with a planetary magnetic field is much more complex and is not completely understood. We shall therefore refrain from any comment on the possible mass interchange which may take place between atmosphere and solar wind.

6. THERMAL STRUCTURE OF THE ATMOSPHERE

In this section we shall investigate the thermal structure for various models of the atmosphere of Mercury. The main purpose is to determine if the exospheric temperature, in any of these models, is low enough for the atmosphere to be stable against gravitational escape. For these calculations we first derive the temperature of the lower atmosphere of Mercury which is assumed to be in radiative equilibrium. We then discuss the region of the mesopause which separates the lower and the upper atmospheres. The calculation of the structure of the thermosphere and exosphere is then presented.

6.1 Atmospheric Models

Four models for the composition of Mercury's atmosphere have been investigated:

(a) Pure argon, as suggested by Field (1964), $P_S = 1$ mb,

(b) 50% argon, 50% carbon dioxide, $P = 5$ mb (atmosphere resulting from outgassing),

(c) 60% carbon dioxide, 25% neon, 15% nitrogen, $P_S = 5$ mb (remnant of primitive atmosphere),

(d) Pure carbon dioxide, as suggested by Moroz (1965), $P_S = 1$ mb.

6.2 Lower Atmosphere and Mesopause

The temperature structure of a planetary atmosphere which is in radiative and convective equilibrium has been discussed in detail by Goody (1964). For an optically thin atmosphere the lower region (troposphere) will be in convective equilibrium and the temperature gradient close to adiabatic. In the upper region (stratosphere) where the optical thickness in the infrared approaches zero, the atmosphere becomes isothermal at $T_o = \frac{T_e}{2^{\frac{1}{4}}} = 438$ $^{\circ}$K.

The values of the adiabatic lapse rate and the height of the tropopause for model atmospheres b, c, and d are given in the first two columns of Table IV. The model a corresponds to a pure argon atmosphere. Being an inert gas, argon is radiatively inactive in the infrared and therefore the optical thickness of the atmosphere is zero. Hence the temperature structure of the lower atmosphere will not be governed by radiation but by conductive and convective processes. As will be shown later, argon will nevertheless absorb the solar ultraviolet in the upper atmosphere, but because of the radiative inertness, this energy will have to be conducted downwards all the way to the surface to be radiated away from the ground. This will probably tend to establish a positive temperature gradient

throughout the atmosphere. For this model, therefore, the temperature profile in the lower atmosphere is highly un-certain, and we shall confine our attention to the exosphere alone, discussed in a later section.

If there are no sources or sinks of energy in the stratosphere, then the temperature for models b, c, and d will remain constant at T_o until the level at which the density becomes so low that LTE breaks down, which is de-noted as the level of vibrational relaxation. At this level in the atmosphere, the radiative lifetime of CO_2 is shorter than the vibrational relaxation time. Assuming a relaxation time for CO_2 of 3 μsec at 420 $^{\circ}K$, the pressure level at which vibrational relaxation will occur is deter-mined to be 8 dynes/cm^2. The height of this level varies with composition, and is also given in Table IV for each model atmosphere.

TABLE IV

MODEL	LAPSE RATE	HEIGHT OF TROPOPAUSE	RELAXATION LEVEL	HEIGHT OF MESOPAUSE	DENSITY OF MESOPAUSE	TEMPERATURE AT MESOPAUSE
b 50% A 50% CO_2 5 mb	5.30 $^\circ$C/km	15.9 km	163 km	200 km	8.2 x 10^{12}	195 $^\circ$K
c 60% CO_2 25% Ne 15% N_2 .5 mb	3.86 $^\circ$C/km	21.5 km	172 km	280 km	12.0 x 10^{12}	200 $^\circ$K
d 100% CO_2 1 mb	4.32 $^\circ$C/km	19.4 km	112 km	150 km	4.9 x 10^{12}	210 $^\circ$K

Above this level, following Chamberlain (1962), the CO_2 emission in the vibration-rotation bands at 15μ is assumed lost to space. The volumetric loss of energy L_v is given by Bates (1951):

$$L_v = \eta \; n(CO_2) Ne^{-h\nu/kT} \; h\nu, \qquad (6)$$

where

η = deactivation coefficient for CO_2,

$n(CO_2)$ = number density of CO_2,

N = total particle number density,

$h\nu$ = quantum energy at 15μ,

T = temperature of CO_2.

With increasing altitude L_v decreases as the product of the number densities, n and N. At the level of the mesopause the total amount of energy radiated from above this height equals the solar ultraviolet energy which is conducted downward from the thermosphere. The temperature gradient at the mesopause is therefore zero. In order to compute the height and number density of individual constituents of the mesopause we need to know the density distribution below. This problem is complicated by the fact that CO_2 is partly photo-dissociated within this region, and a layer of O_2 may form which in turn may screen CO_2

from the solar ultraviolet radiation. Marmo and Warneck (1961) have studied a similar problem for Mars. Following their procedure we first obtain the photochemical equilibrium distribution with height for CO_2, O_2, O and CO in this region. Using these numbers we then derive the height, density and temperature at the mesopause for each model. The results are shown in Table IV.

6.3 Thermosphere and Exosphere

The temperature distribution above the mesopause is determined by the heat conduction equation,

$$\frac{d}{dz}\left(\varkappa \frac{dT}{dz}\right) = Q - L, \tag{7}$$

where Q is the amount of solar ultraviolet and x-ray energy absorbed per unit volume, L is the energy radiated per unit volume, and $\varkappa$ is the thermal conductivity.

The input of the solar energy in the thermosphere in each model atmosphere is mainly due to absorption of ultraviolet radiation by CO, O and by Ne or A. This is because CO_2 is mostly dissociated at lower levels, near the mesopause. It is also assumed that above the mesopause diffusive separation occurs and the density distribution of each constituent is determined by its own scale height. Because of

- 29 -

this circumstance, the solar energy deposited in the thermosphere is due to the absorption of the ionizing radiation of wavelengths less than 900 Å. Not all of this solar energy goes into heating. Walker (1964) has made a detailed study of the efficiency of heating at different altitudes in the earth's atmosphere. Using his results, we adopt a mean efficiency (ϵ) of 50 percent for the conversion of solar ultraviolet to heat. The other half is radiated away and/or carried to lower levels by downward diffusion. Therefore the expression for Q for a slowly rotating planet, is

$$ Q = \frac{1}{2} \epsilon \left[\int_{\lambda_1}^{\lambda_2} F_\infty(\lambda) e^{-\tau(\lambda z)} d\lambda \right] \sum_i n_i(z) \sigma_i \qquad (8) $$

where

ϵ = efficiency of conversion of solar ultraviolet to heat

F_∞ = incident solar flux

τ = optical thickness

λ = wavelength

z = altitude

n_i = number density of the ionizing constituent

σ = ionization cross section.

The radiative loss term, L, in Eq. (7) represents the total radiation per unit volume emitted by the atmosphere

that is lost to space. As such, this is valid for the at-
mosphere above some level where the optical thickness is
small and the absorption of radiation by the atmosphere
above is negligible. For the atmospheric models under con-
sideration, the emission is mainly by CO_2 in the 15 μ vibra-
tion-rotation band, and CO in the 4.66 μ band. The emission
by atomic oxygen at 63 μ is assumed negligible.

High up in the thermosphere, where the temperature
reaches a maximum, the term L is dominated by emission of
CO. The energy L_r radiated per unit volume by CO (4.66 μ
band) is given by Bates (1951):

$$L_r = 0.26(kT)^2 \, B^2 \, P^2 \, n(CO) \; ev/cm^3/sec \; , \quad (9)$$

where

$$B = \text{rotation constant of CO}$$

$$P = \text{dipole moment of CO}$$

$$T = \text{temperature}$$

$$n(CO) = \text{number density of CO.}$$

From the above expression it is seen that emission due to
CO increases as T^2 which results in the dominance of CO
radiation at high altitudes.

The level at which CO emission becomes important de-
pends on the mean optical thickness of the rotation lines.

McElroy, L'Ecuyer and Chamberlain (1965) have suggested that the height at which the optical thickness of the lines equals unity is the level above which CO radiation is dominant. Below this level CO_2 is the principal radiator and L is given by L_v (Eq. (6)). But for calculating the exospheric temperatures, L can be replaced by L_r in models b, c, and d. As model a only consists of an argon atmosphere, L = 0.

The exospheric temperature can now be determined by solving the integro-differential equation (7) by a convergent iterative process. The first order solution for the exospheric temperature, T_∞, is obtained from the following expression:

$$\frac{A}{p+1}\left[T_\infty^{p+1} - T_m^{p+1}\right] = \frac{1}{2}\ \epsilon F \Delta\lambda H_i \left[0.5772 + \ell n\ \tau_m + E_i(\tau_m) - \frac{H_{CO_2}}{H_i}\right]$$

$$- Cn_r(CO)T_r^2H_r^2(CO)\left[1 + \frac{Z_r - Z_m}{H_r}\right] \qquad (10)$$

In this equation,

T_m = mesopause temperature

A = conductivity coefficient in $\varkappa = AT^p$

p = exponent of the temperature dependence of $\varkappa$

F = average incident solar flux over the spectral band $\Delta\lambda$

$$\Delta\lambda = 900 - 44 \text{ Å} \quad (856 \text{ Å})$$

τ_m = mean optical thickness of the atmosphere at the mesopause to ionizing radiation

$E_i(\tau m)$ = exponential integral

H_{CO_2} = scale height of CO_2 at the mesopause

H_i = scale height of the principal ionized constituent (O or Ne) in the vicinity of the level of maximum absorption,

C = constant = $0.26 \, K^2 B^2 P^2 = 2.9 \times 10^{-23}$

z_m = mesopause altitude,

and the subscript r denotes the level at which the optical thickness of the CO rotation lines equals unity.

If we assume that the level z_r is high enough to make $T_r \approx T_\infty$, then $H_r = kT_\infty/mg_r$, where g_r is the gravitational acceleration at $z = z_r$ and m now corresponds to the molecular weight of CO. Also, it is assumed that the level of maximum absorption of solar ionizing radiation occurs at an altitude high enough to make $H_i \approx kT_\infty/m_i g$, where m_i is the molecular weight of the principal ionizing particle. With these assumptions, we solve Eq. (10) for the exospheric temperature T_∞ for each of the atmospheric models. The results are shown in Table V.

TABLE V

EXOSPHERIC TEMPERATURE

Model	Composition	Exospheric Temperature
a	100% A	$> 10,000\ ^{\circ}K$
b	50% CO_2 50% A	$1100\ ^{\circ}K$
c	60% CO_2 25% Ne 15% N_2	$1050\ ^{\circ}K$
d	100% CO_2	$1100\ ^{\circ}K$

As mentioned above, these temperature values have been calculated on the assumption that $H_i \approx H_r \approx H_\infty$. However, the uncertainty in the exact level at which cooling by CO becomes effective and the level at which the maximum absorption of energy due to ionization occurs is large, and results in a wide range of values for the exospheric temperature. Also, there is considerable uncertainty in the magnitude of the solar ultraviolet flux and in the exact value of the heating efficiency factor ϵ. With these limitations in mind,

it is perhaps worthwhile to emphasize that, depending on

the assumptions made, the exospheric temperature of Mercury

for models $\underline{b}$, $\underline{c}$ and $\underline{d}$ can be as high as 1800 $^\circ$K or as low

as 800 $^\circ$K.

6.4 Discussion

There are two main conclusions that can be drawn

from the results of Section 6.3:

(1) A pure argon atmosphere cannot be stable against

gravitational escape. At $T_c > 10,000$ $^\circ$K, argon will escape

in a relatively short time.

(2) If the observations of Moroz are correct and CO_2

is present in the atmosphere of Mercury, then enough CO is

produced in the upper atmosphere by photodissociation so

that the exospheric temperature in each of the three models

$\underline{b}$, $\underline{c}$ and $\underline{d}$ will be in a range that will still permit an at-

mosphere that is stable against thermal escape. The large

margin of error, 800 $^\circ$K to 1800 $^\circ$K, is mainly because of the

uncertainty in the value of the solar ultraviolet flux, the

efficiency factor, and the scale heights at which CO emission

becomes dominant and the absorption of ionization energy is

maximum.

It is interesting to note that despite the large

differences in the molecular weight and thermal conducti-
vity of argon and neon, models b and c give approximately
the same temperature at the top of the atmosphere. This
result is brought about because of the basic assumption
that above the mesopause the atmosphere is in diffusive
equilibrium and therefore, in all three models b, c and d,
at the top of the atmosphere, atomic oxygen becomes the
dominant constituent and the principal absorber of the ionizing
radiation. Also, at high temperatures, the emission by CO
is so intense that very little energy is available to be
conducted down, and therefore the thermal conductivity of
gases does not play an important role in determining the
exospheric temperature. Only the temperature gradient in
the thermosphere is affected, which in turn modifies the
height of the exosphere. However, the changes are small and
will not considerably alter our calculations of the flux of
escaping gases.

It may also be pointed out that these calculations of
the exospheric temperature do not take into account any ef-
fect of the transport of heat by circulation in the upper
atmosphere.

The implication of these results appears to be that if
the actual temperature of the exosphere of Mercury is close

to our calculated lower limit, i.e., $\sim 800\ ^oK$, then models $\underline{b}$, $\underline{c}$ and $\underline{d}$ are stable against gravitational escape. In this case the observed CO_2 may be of primordial origin and the atmosphere may contain substantial proportions of neon. However, one cannot rule out the possibility of accumulating an atmosphere by outgassing also. If, on the other hand, the average exospheric temperature is higher than $800\ ^oK$ but less than $1200\ ^oK$, then both O and Ne will escape and the atmosphere will be mainly CO and A. Molecules of CO may recombine to form CO_2, but the process is not presently understood. If the exospheric temperature were to be between 1300 and $1800\ ^oK$, then even CO would be lost, resulting in an atmosphere composed mainly of argon and of that amount of CO_2 which will be in equilibrium between outgassing from the interior and gravitational escape from the top of the atmosphere.

In summary, therefore, it is suggested that the presence of CO_2 in the atmosphere of Mercury is not only highly probable, but is an essential condition for any substantial amount of atmosphere to exist on the planet.

ACKNOWLEDGMENTS

REFERENCES

Adams, W.S. and T. Dunham, Jr. (1932): Publ. Astron. Soc. Pacific 44, 243.

Antoniadi, E.M. (1934): La Planète Mercure (Paris: Gauthier Villars).

Bates, D.R. (1951): Proc. Phys. Soc. London B 64, 805.

Baum, R.M. (1960): in A Guide to the Planets by P. Moore (New York: Norton and Co., Inc.), plate II.

―――――. (1963): in The Planet Mercury by W. Sandner (New York: MacMillan Co.).

Cameron, A.G.W. (1963): Yale University Lecture Notes, 1962-63, compiled by W.D. Arnett, C.J. Hansen, and J.W. Truran.

Chamberlain, J.W. (1962): Ap. J. 136, 582.

Chamberlain, J.W. and D. Hunten (1965): Rev. of Geophys. 3, 299.

Colombo, G. (1965): Nature 208, 575.

Dollfus, A. (1953): Bull. Soc. Astron. France 67, 61.

―――――. (1957): Ann. d'Astroph. Supp. 4.

―――――. (1961): in Planets and Satellites: Solar System III, G.P. Kuiper and B.N. Middlehurst, eds. (Chicago: University of Chicago Press).

―――――. (1962): in Handbuch der Physik (Berlin: Springer-Verlag), Vol. 54.

Field, G. (1964): in The Origin and Evolution of the Atmospheres and Oceans, P.J. Brancazio and A.G.W. Cameron, eds. (New York: J. Wiley and Sons, Inc.)

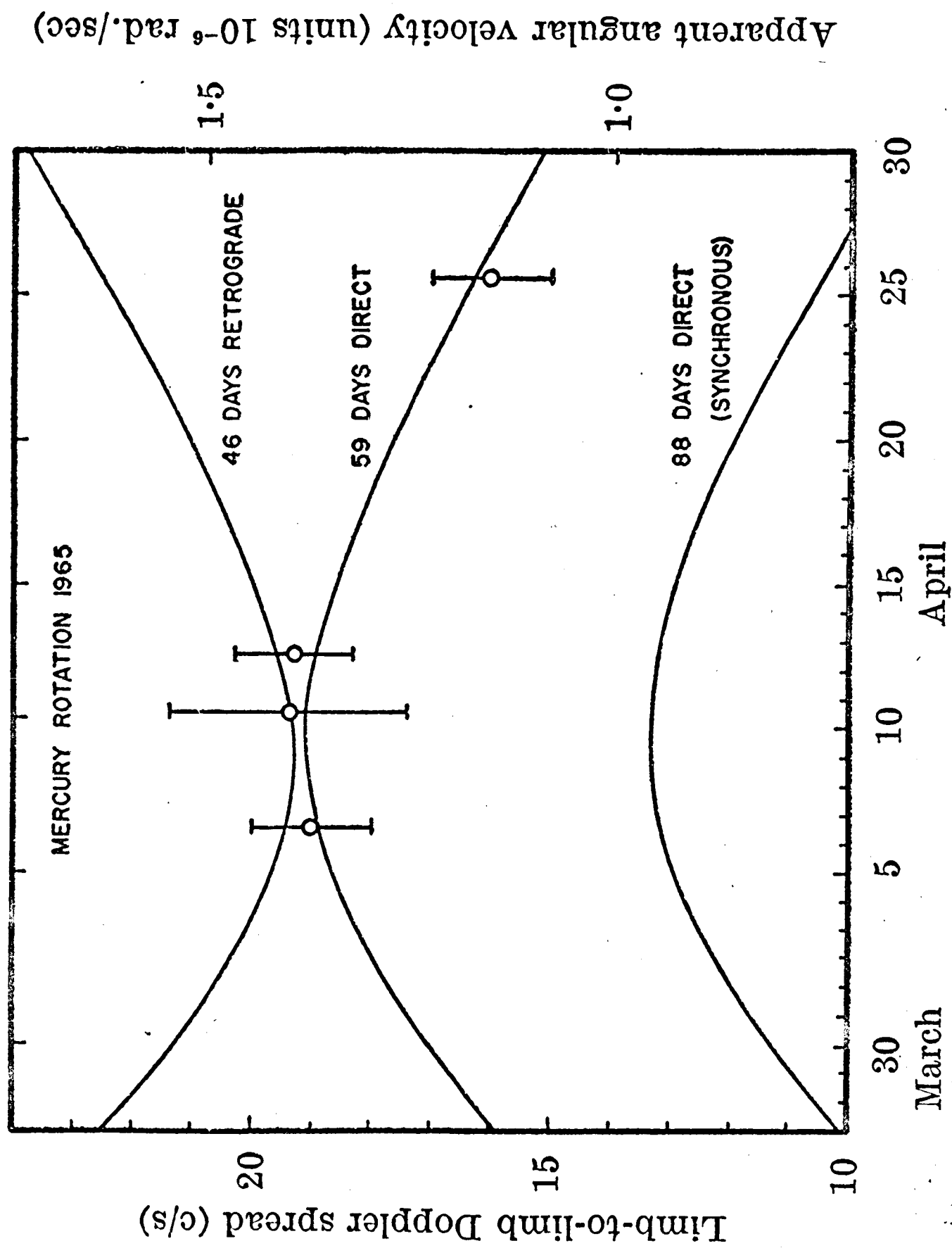Goody, R.M. (1964): Atmospheric Radiation (Oxford: Clarendon Press).

Harris, D.L. (1961): in _Planets and Satellites: Solar System III_, G.P. Kuiper and B.N. Middlehurst, eds. (Chicago: University of Chicago Press).

Hintereggar, H.E. (1961): J. Geophys. Res. 66, 2367.

Howard, W.E. III, A.H. Barrett and F.T. Haddock (1962): Ap. J. 136, 995.

Jeans, J.H. (1916): _Dynamical Theory of Gases_ (New York: Dover Publication, 1954).

Kellerman, K.I. (1965): Nature 205, 1091.

Kozyrev, N.A. (1964): Sky and Telescope XXVII, 339.

Kuiper, G.P. (1952): in _Atmospheres of the Earth and Planets_, G.P. Kuiper, ed. (Chicago: University of Chicago Press).

Lowell, P. (1902): Mem. Amer. Acad. Arts and Sci. 12, 431.

Lyot, B. (1929): Ann. de l'Observatoire de Paris, Section de Meudon, Vol. VIII. NASA translation TT F-187, July 1964.

————. (1943): Astronomie 67, 3.

Marmo, F.F. and P. Warneck (1961): Final Report, Contract Nas w-124, Geophysics Corporation of America, Bedford, Massachusetts.

Mayer, C.H. (1961): in _Planets and Satellites: Solar System III_, G.P. Kuiper and B.N. Middlehurst, eds. (Chicago: University of Chicago Press).

McElroy, M.B., J. L'Ecuyer and J.W. Chamberlain (1965): Ap. J. 141, 1523.

McGovern, W.E., S.H. Gross and S.I. Rasool (1965): Nature 208, 375.

Mintz, Y. (1962): Icarus 1, 172.

Moroz, V.I. (1963): Astr. Tsirk (USSR), No. 270.
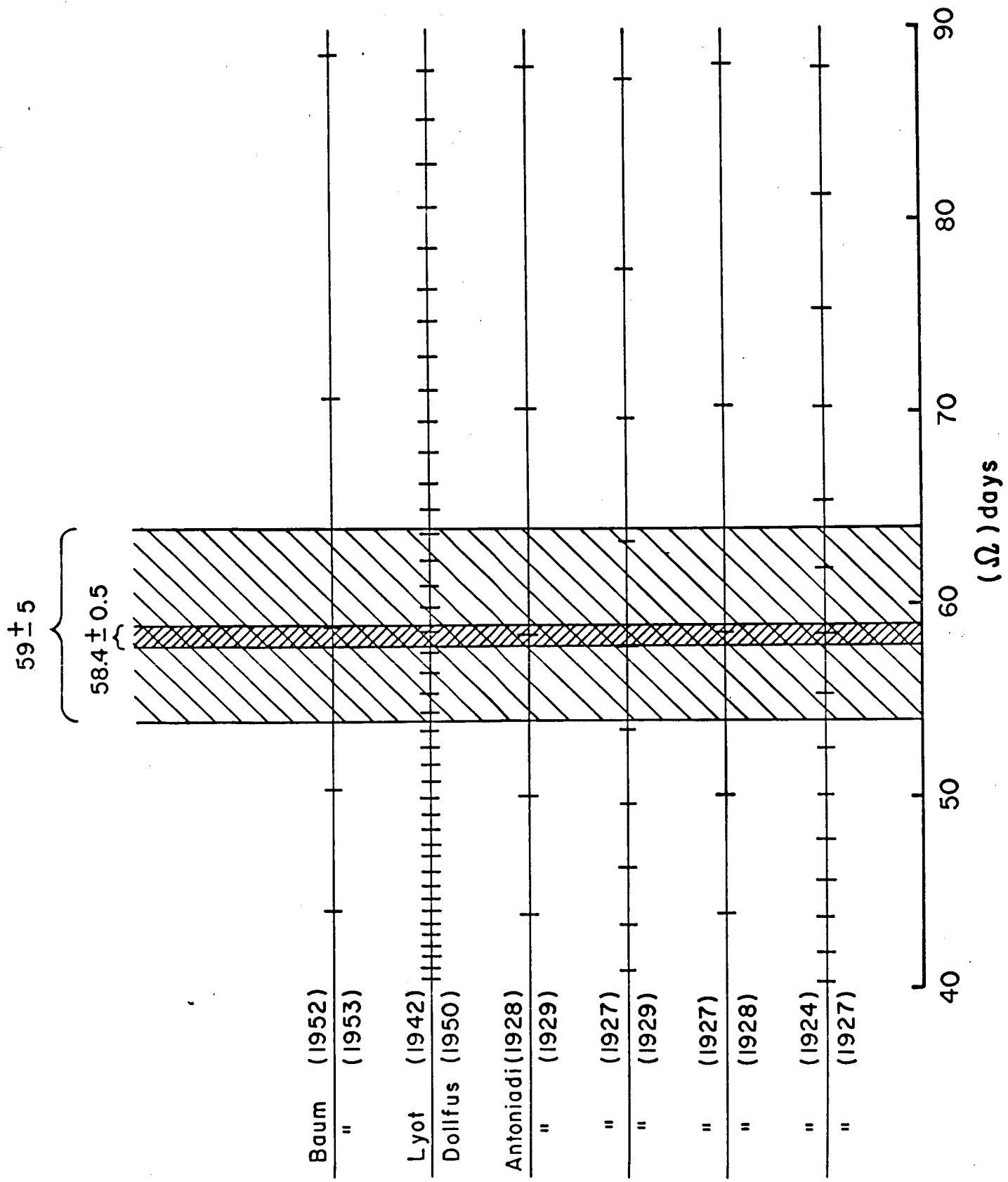
Moroz, V.I. (1965): Soviet Astronomy-AJ 8, 882.

Opik, E.J. (1961): J. Geophys. Res. 66, 2808.

Peale, S.J. and T. Gold (1965): Nature 206, 1240.

Pettengill, G.H. and R.B. Dyce (1965): Nature 206, 1240.

Pettit, E. (1961): in Planets and Satellites: Solar System III, G.P. Kuiper and B.N. Middlehurst, eds. (Chicago: University of Chicago Press).

Schiaparelli, G.V. (1889): Astron. Nachr. 123, 241.

Spinrad, H., G. Field and P. Hodge (1965): Ap. J. 141. 1155.

Spinrad, H. and P. Hodge (1965): Icarus 4, 105.

Spitzer, L. Jr. (1952): in Atmospheres of the Earth and Planets, G.P. Kuiper, ed. (Chicago: University of Chicago Press).

Urey, H.C. (1959): in Handbuch der Physik (Berlin: Springer-Verlag), Vol. 52.

Walker, J.C.G. (1961): Ap. J. 133, 274.
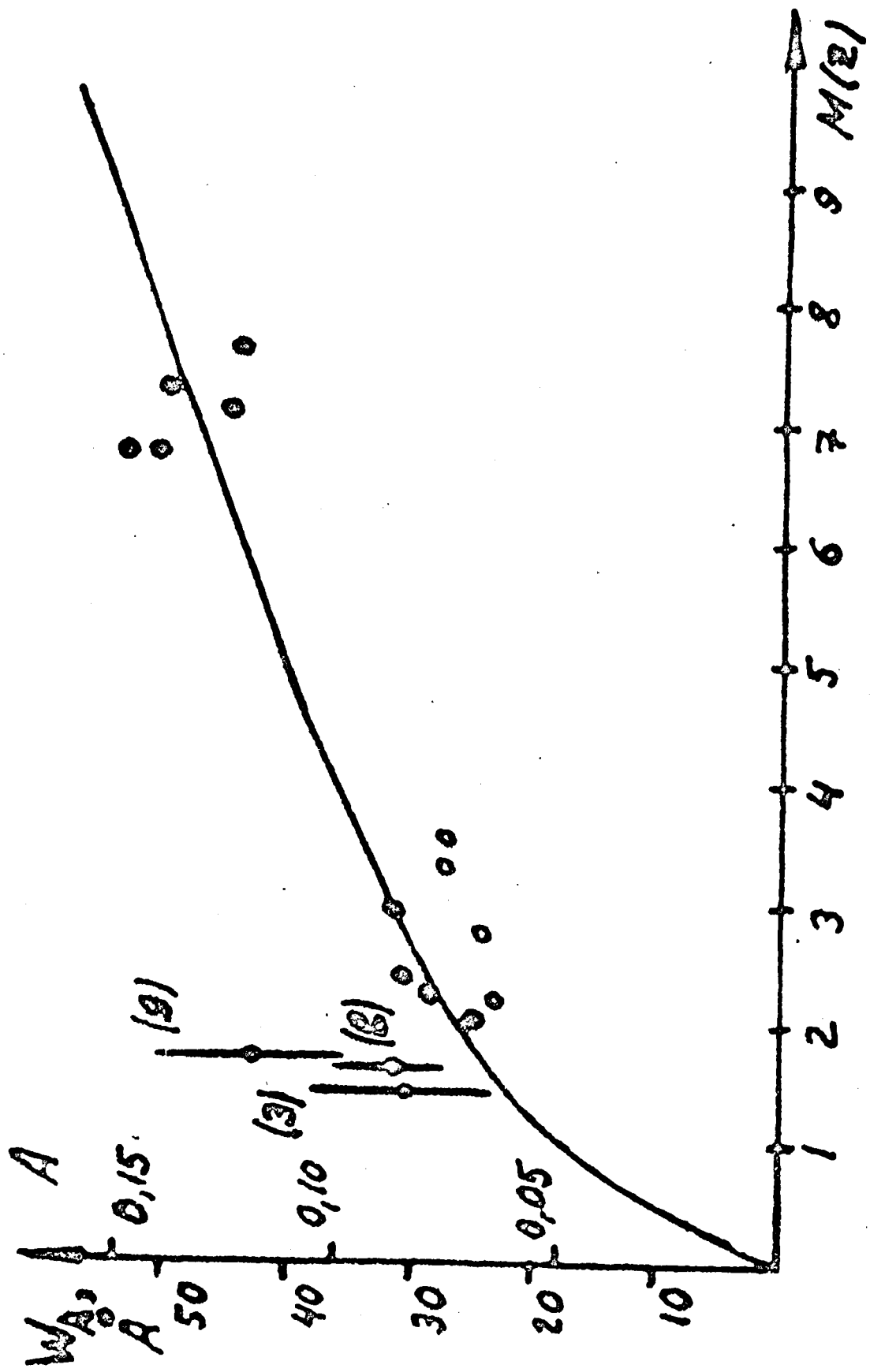
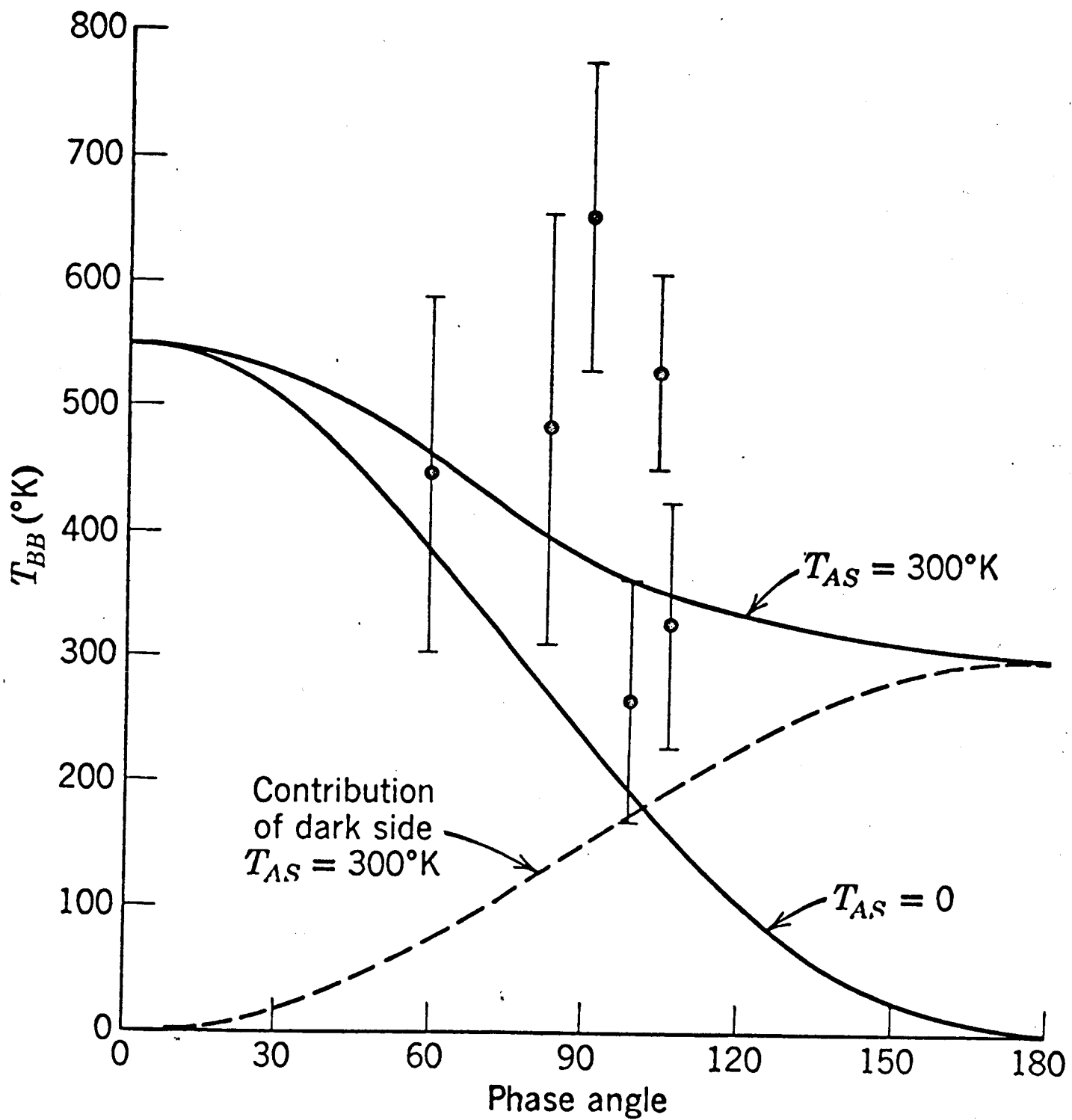—————————. (1964): Dissertation, Columbia University.

FIGURE CAPTIONS

Figure 1: Plot of the apparent rotational angular velocity
of the planet Mercury versus date for several
values of rotation during the inferior conjunc-
tion of April 1965. The values inferred from
the measurements are shown with their estimated
errors (after Pettengill and Dyce, 1965).

Figure 2: Rotation periods of the planet Mercury, in days,
as derived from six pairs of drawings. The
single-hatched area shows the limits in the
rotation period allowed by the radar observations
of Mercury. Visual observations indicate a value
of 58.4 ± 0.5 (double-hatched area).

Figure 3: The total equivalent width of CO_2 bands at 1.59 μ
in the spectrum of Mercury ($\dagger$) and the sun (o).
The figure in parentheses indicates the number of
observations on which the value is based. The
solid curve is the theoretical curve of growth
for CO_2 absorption in the earth's atmosphere
(after Moroz, 1963).

Figure 4: Computed apparent blackbody temperatures of
Mercury at centimeter wavelengths. Lower
solid curve (B) applies if dark side is cold.
Upper solid curve (A) includes contribution
of dark side at 300 °K (after Field, 1964).

Figure 5: Equivalent blackbody disk temperature of
Mercury as a function of planetocentric phase
angle. The solid line shows the expected phase
law for a smooth non-rotating planet with no
atmosphere and a low thermal conductivity. The
curve shown corresponds to a sub-solar tempera-
ture of 610 °K and it is assumed that there is
no source of heat other than solar radiation
(after Kellerman, 1965.).

Figure 6: The required wind velocities as a function of
temperature increase on the dark side of the
planet Mercury. V_s = velocity of sound in the
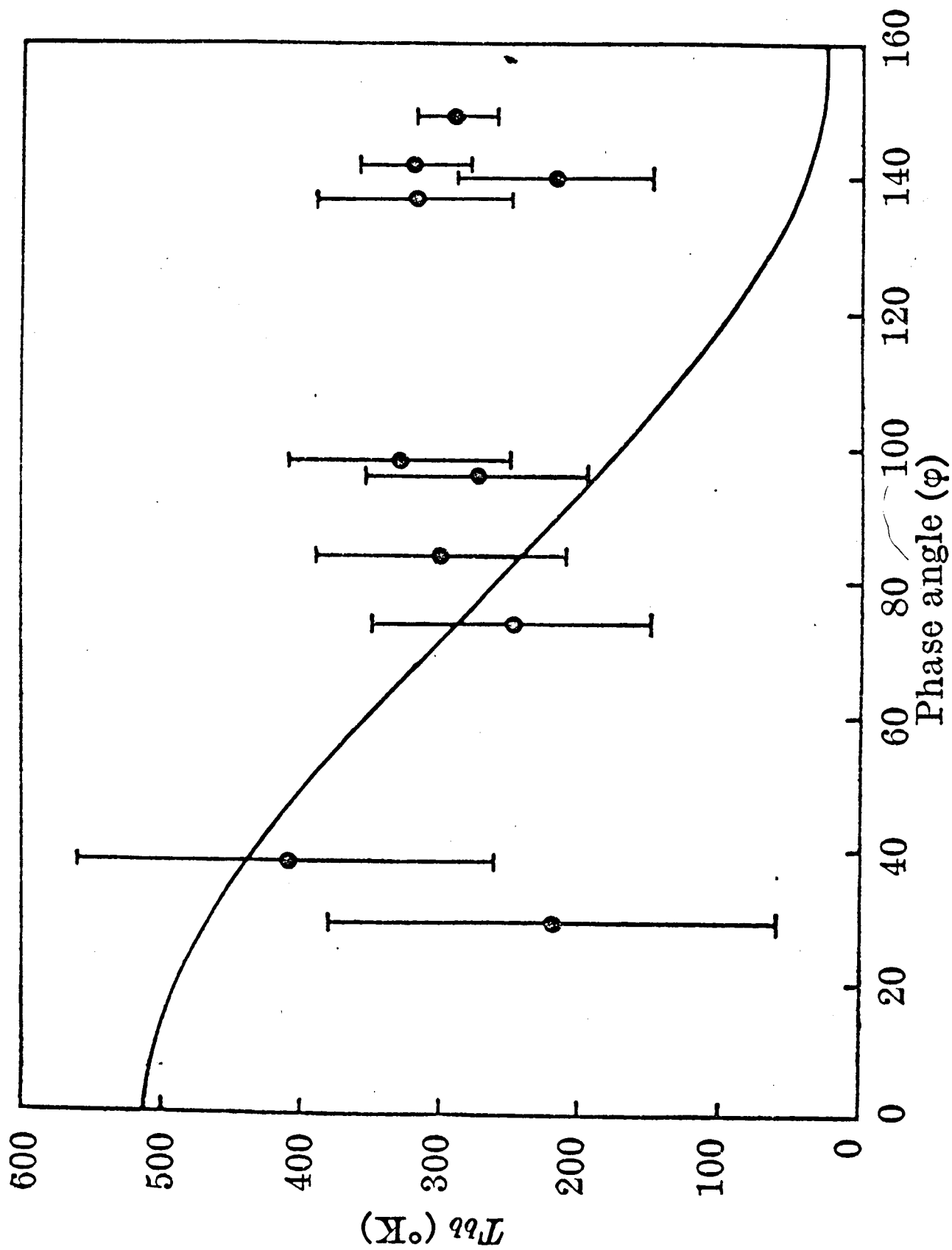atmosphere at these temperatures.

Figure 7:   The time of escape of gases from the planet Mer-
            cury as a function of atomic or molecular weight
            of the escaping particles.

Apparent angular velocity (units 10^{-6} rad./sec)

Limb-to-limb Doppler spread (c/s)

MERCURY ROTATION 1965

46 DAYS RETROGRADE

59 DAYS DIRECT

88 DAYS DIRECT (SYNCHRONOUS)

March   April

1·5   1·0

20   15   10

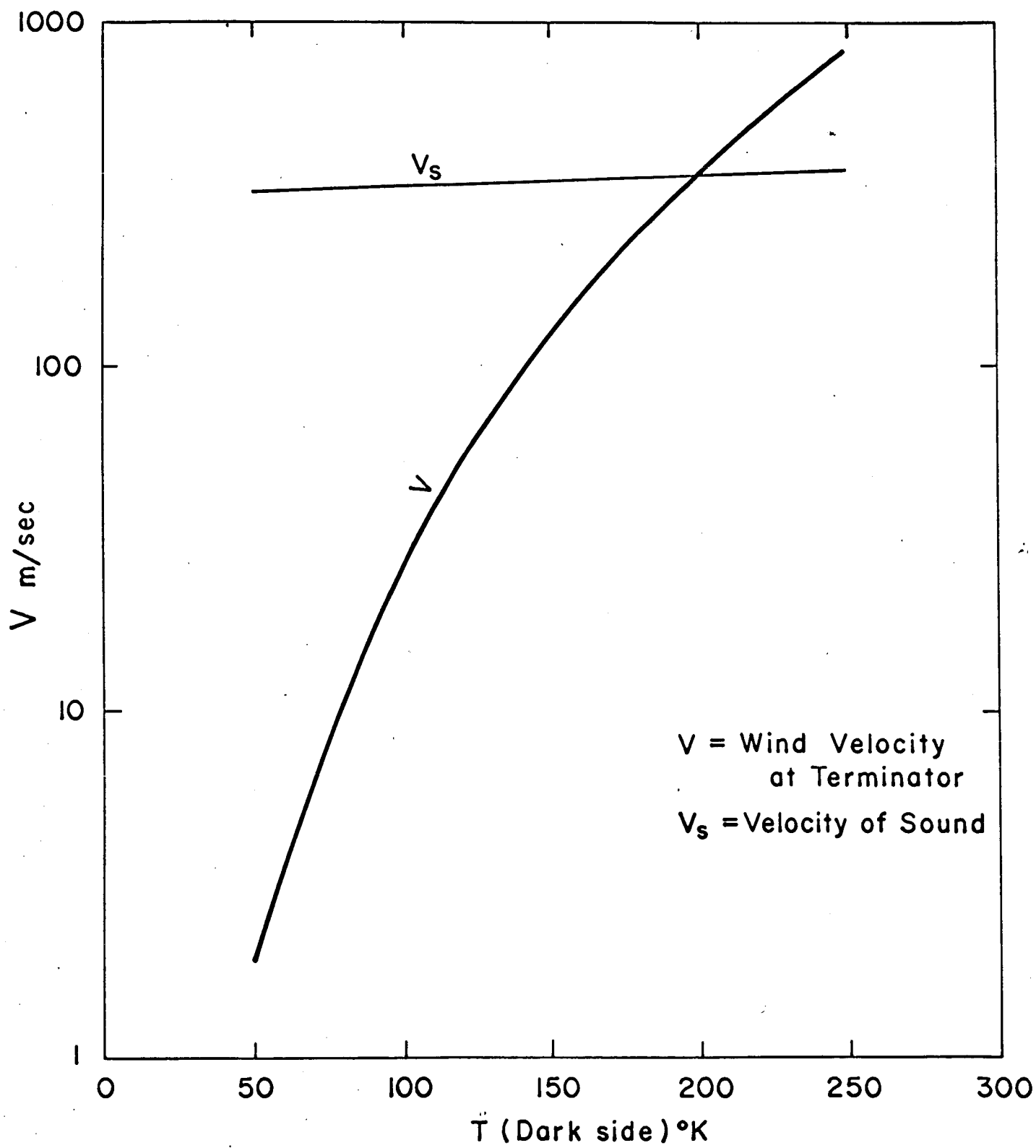30   5   10   15   20   25   30

Phase angle (φ)

T_{bb} (°K)

Time of Escape of Gases from the Planet Mercury